International Journal of Heat and Mass Transfer 128 (2019) 762–772

Contents lists available at ScienceDirect

International Journal of Heat and Mass Transfer

journal homepage: www.elsevier.com/locate/ijhmt

Effects of magnetic field on the pool boiling heat transfer of water-based α-Fe_2O_3 and γ-Fe_2O_3 nanofluids

Shi-Yan Li, Wen-Tao Ji *, Chuang-Yao Zhao, Hu Zhang, Wen-Quan Tao

Key Laboratory of Thermo-Fluid Science and Engineering of MOE, Xi'an Jiaotong University, Xi'an 710049, China

ARTICLE INFO

Article history:
Received 18 March 2018
Received in revised form 2 September 2018
Accepted 6 September 2018
Available online 17 September 2018

Keywords:
Pool boiling
Magnetic field
Ferric oxide nanoparticles
Heat transfer enhancement

ABSTRACT

Pool boiling experiments of water-based α-Fe_2O_3 and γ-Fe_2O_3 nanofluids with different concentrations (0.005–0.100 g/L) were conducted at atmospheric pressure. Two kinds of magnetic field induced by two neodymium magnets were also applied to investigate the effects of magnetic field on the pool boiling of nanofluids. It demonstrated that the magnetic field could change the local concentration of nanofluids and produce an extra pressure on the bubble boundary. The extent of the effects was not only dependent on the intensity and distribution of magnetic field, but also the magnetism and concentration of nanoparticles. For the 0.050 g/L γ-Fe_2O_3 nanofluid in the presence of magnetic field induced by two mutually exclusive magnets, an enhancement in boiling heat transfer coefficient up to 28% was obtained. The results of the experiments indicated the feasibility to control the pool boiling performance of magnetic nanofluids by external magnetic field.

1. Introduction

With the development of products with higher heat flux, the heat dissipation requirement is more prominent. As one of the most effective heat transfer methods, boiling has been widely used in industry. In recent decades, many studies have focused on the improvement of boiling heat transfer coefficient and critical heat flux from different aspects [1,2]. Among them, adding nanoparticles is more attractive because the nanofluids might exhibit superior properties in pool boiling heat transfer.

Various nanoparticles were used to investigate the effects of nanoparticles on pool boiling, such as Al_2O_3 [3–5], TiO_2 [6,7], SiO_2 [8,9] and carbon nanotubes [10,11]. However, these experimental results varied from one to another. Many factors are correlated with the results of nanofluids pool boiling experiments, including the size, type, wettability and concentration of the nanoparticles [4,7,8,12,13,14], the roughness of heat surface and heat flux [15,16].

Investigations on the boiling of magnetic nanofluids were also performed in recent years. Magnetic nanofluids are suspensions which are comprised of a non-magnetic base fluid and magnetic nanoparticles. Table 1 shows the previous pool boiling experiments on magnetic nanofluids [13–15,17–20]. Although the results of magnetic nanofluids were similar to those of conventional nanofluids, they could exhibit some special features in the presence of magnetic field. Ishimoto et al. [21] investigated the behavior of single bubble in magnetic nanofluid under nonuniform magnetic field. They found that the velocity of single bubble in magnetic nanofluid could be influenced by external magnetic field due to the magnetic body force. The fundamental study on bubble behavior indicated that it was possible to control the boiling process of magnetic nanofluid by external magnetic field. Lee et al. [22] studied the effects of nanoparticles on the CHF enhancement using a Ni-Cr wire in pool boiling. It indicated that the CHF of Fe_3O_4/water nanofluid showed the highest value compared with Al_2O_3 and TiO_2 nanofluids. The Biot-Savart law was applied to analyze the effects of magnetic field induced by electrical current on CHF. They speculated that more Fe_3O_4 nanoparticles would deposit on the wire and the local concentration could be changed by the effect of magnetic field. Khoshmehr et al. [23] tested the quenching process of Fe_3O_4/water nanofluid with the implementation of magnetic field. The directional movement of nanoparticles in nanofluid was validated by Particle Image Velocimetry technique, which could provide supporting evidence for the assumption proposed by Lee et al. [22].

There were relatively few studies available on the effect of magnetic field on boiling heat transfer of nanofluid [20,24,25,26,27]. Liu et al. [24] placed a ring permanent magnet at the bottom of boiling vessel to investigate the mechanism of boiling heat transfer enhancement of water-based magnetic fluid with and without magnetic field. They explained the enhancement on boiling heat

* Corresponding author.
E-mail address: wentaoji@xjtu.edu.cn (W.-T. Ji).

https://doi.org/10.1016/j.ijheatmasstransfer.2018.09.022
0017-9310/

Nomenclature

List of symbols

B	magnetic flux density, T (1 T = 10^4 G)
c_p	specific heat capacity, J/kg·K
C_{wl}	an empirical constant in Rohsenow correlation [32]
F_m	magnetic force, N
g	gravitational acceleration, m/s^2
h	heat transfer coefficient, W/m^2·K
H	magnetic field intensity, A/m
M	magnetization, A/m
p	pressure, Pa
Pr	Prandtl number
q	heat flux, W/m^2
r	Latent heat, J/kg
Ra	average roughness of heat surface, μm
s	an empirical constant in Rohsenow correlation [32]
T	temperature, °C
ΔT	superheat temperature
x	distance, m

Greek alphabet

η	dynamic viscosity, Pa·s
λ	thermal conductivity, W/m·K
μ	vacuum permeability
ρ	density, kg/m^3
σ	surface tension, N/m
ϕ	heat loss rate
χ	volume susceptibility

Subscript

l	liquid
n	nanoparticle
sat	saturation
v	vapor
w	wall

transfer coefficient by analyzing the magnetic levitation force acting on a single bubble. Sesen et al. [25] studied the pool boiling of Fe_3O_4/water nanofluid with the magnetic field provided by magnetic stirrers. An enhancement on boiling heat transfer coefficient of 17% was achieved by magnetic actuation, they reported that the magnetic field intensified the circulations and mixing in nanofluid. Abdollahi et al. [20] investigated the influence of magnetic field induced by two magnets on Fe_3O_4/water nanofluid, they found that the diminution or increment of boiling heat transfer coefficient was dependent on the simultaneous effect of magnetic field on both the base fluid and the nanoparticles. The effect of magnetic field on the base fluid was due to the magnetic body force on the bubbles, the direction of which was opposite to that of magnetic field gradient. Shojaeian et al. [26] studied the pool boiling of Fe_3O_4 nanofluids under a rotating magnetic field. It was reported that the magnetic actuation could prevent the sedimentation of nanoparticles and assist the circulation of magnetic nanoparticles in nanofluids. Ozdemir et al. [27] investigated the pool boiling of Fe_3O_4 nanofluids with magnetic actuation experimentally. They found that the magnetic actuation could enhance the boiling heat transfer significantly. In addition, it was reported that the effect of concentration was insignificant when the magnetic actuation was adopted.

Although many researchers have mentioned the effects of magnetic field on pool boiling of magnetic fluids, it is still far from being adequate to the facts. Especially when a magnetic field exists, the effect of nanoparticle concentration on boiling heat transfer needs further research. In addition, many magnetic nanofluids used in previous research contain surfactant or the nanoparticles are coated with other materials, it will change the force between nanoparticles and make the analysis more complicated. Considering that the Fe_3O_4 nanoparticle was highly susceptible to oxidation when exposed to atmosphere [28], α-Fe_2O_3 and γ-Fe_2O_3/water nanofluids with rather low concentrations were used to investigate the effects of magnetic field on pool boiling heat transfer. The joint effect of external magnetic field and nanoparticles on pool boiling was analyzed. Moreover, the study evaluated the feasibility of controlling the pool boiling process of magnetic nanofluids by external magnetic field.

2. Experimental apparatus and procedure

2.1. Experimental setup

A schematic diagram of the pool boiling test setup is shown in Fig. 1. The setup consisted of four main parts. It includes boiling

Table 1
Summary of the pool boiling experiments on magnetic nanofluids.

Reference (year)	Heating surface	Nanofluids and concentration	Nanoparticle size	Results of boiling heat transfer coefficient
Stutz et al. [17]	100 μm diameter platinum wire	γ-Fe_2O_3/water 0.1 wt%	10 nm	Deterioration or enhancement based on coating duration
Sheikhbahai et al. [18]	Ni-Cr wire	Fe_3O_4/EG-water 0.01–0.1 vol%	50 nm	Deterioration
Souza et al. [13]	Copper disc of 12mm diameter	γ-Fe_2O_3/HFE7100 0.29 g/L	10, 80 nm	Deterioration or enhancement based on nanoparticle size
Salari et al. [19]	Copper disc of 11 mm diameter	Fe_3O_4/water 0.1–0.3 wt%	20 nm	Enhancement
Kiyomura et al. [14]	Copper block of 20 mm diameter	γ-Fe_2O_3/water 0.029, 0.29 g/L	10 nm	Deterioration or enhancement based on surface roughness and concentration
Abdollahi et al. [20]	Copper block of 45 mm diameter	Fe_3O_4/water 0.01–0.4 vol%	25 nm	Enhanced at low concentration, deteriorated at high concentration
Salimpour et al. [15]	Copper block of 45 mm diameter	Fe_3O_4/water 0.5 vol%	25 nm	Deterioration or enhancement based on surface roughness and heat flux

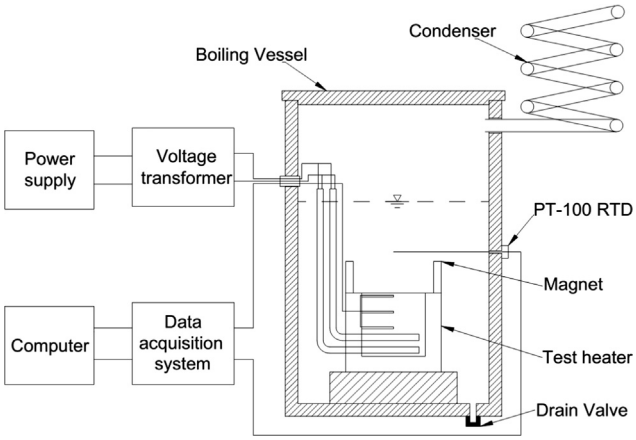

Fig. 1. Schematic of the apparatus.

vessel, test heater, data acquisition system and magnets. The cylindrical vessel for boiling was made from stainless steel, and it had the height of 50 cm and inner diameter of 30 cm. A spiral double-side enhanced copper tube was installed at the top of the vessel to minimize the loss of working fluid and maintain atmospheric pressure in the vessel. A drain valve was installed at the bottom of the vessel. Two observation windows with the diameter of 80 mm were also installed in the vessel. The vessel were all well insulated with rubber plastic and aluminum foil to prevent the heat loss.

Fig. 2 presents the schematic of the test heater used in this study. The test heater consisted of a copper block, nine T-type thermocouples, eight cartridge heaters and the insulating adhesive. The copper block was a cube with a length of 100 mm. The purity of copper was more than 99.9%. It had eight holes with inner diameter of 10.2 mm and nine small holes with inner diameter of 3 mm. The location of these holes is shown in Fig. 3. Eight cartridge heaters with outer diameter of 10 mm were inserted into the copper block, and every cartridge heater was wrapped with copper foil

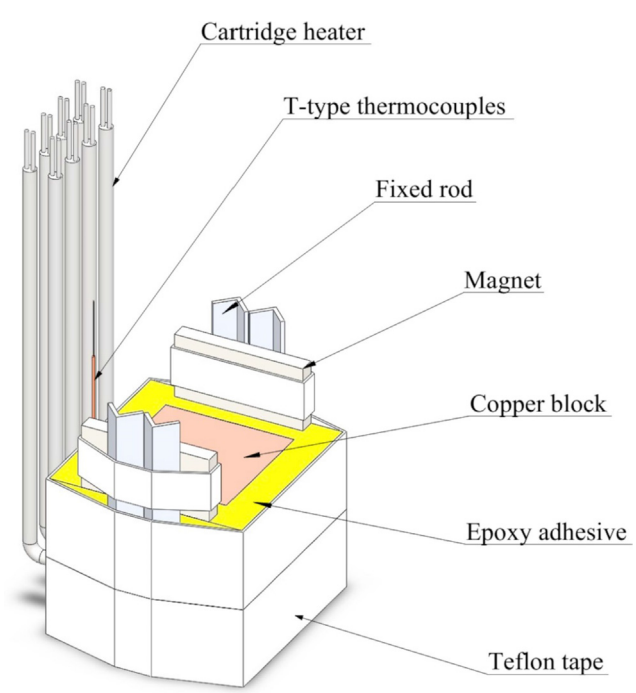

Fig. 2. Schematic of the test heater.

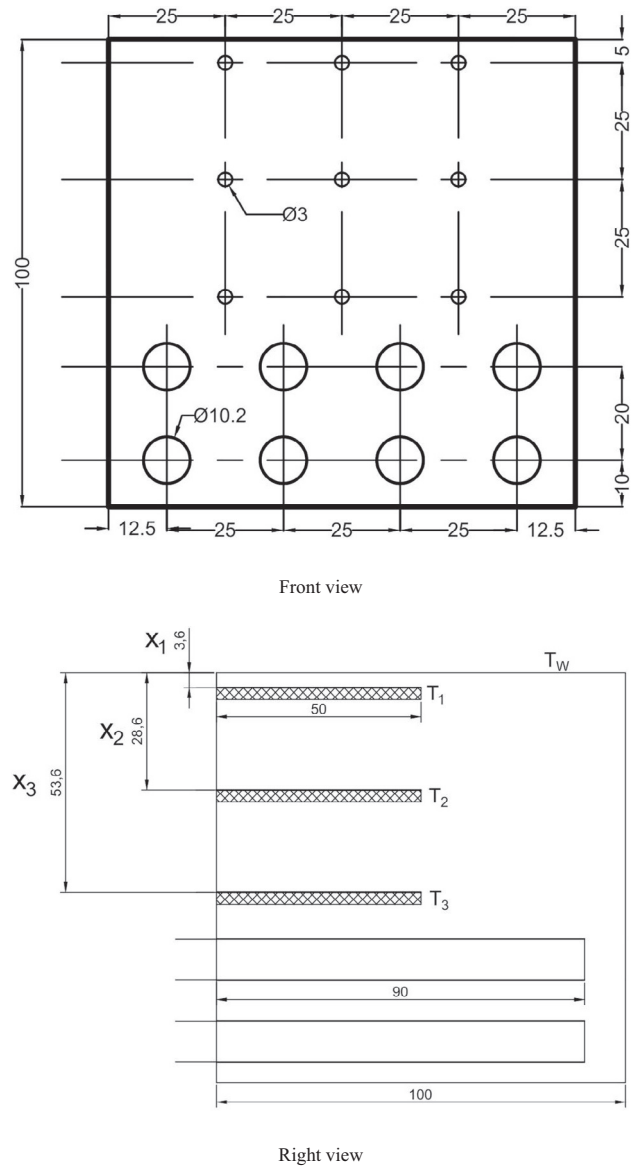

Fig. 3. Location of thermocouples and cartridge heaters (Unit: mm).

to reduce the contact thermal resistance. The resistance wire of every cartridge heater has a length of 8 cm and it is totally in the copper block. The voltage of every heater was controlled by a voltage transformer to provide various levels of output power. To obtain the wall temperature and the heat flux, nine T-type thermocouples with diameters of 0.2 mm clung to the upper wall of these small holes to measure the temperatures of different points in the copper block. Using a copper rod with diameter of 2.5 mm and some copper wires, the thermocouple wires were pushed and firmly attached to the upper surfaces of the small holes. To minimize the contact thermal resistance, more copper wires and powder were used to fill the holes. In addition, the thermocouple wires were kept straight forward when entering the small holes. The position were accurately fixed and winding was not allowed in the mounting process. The insulating adhesive was made using epoxy adhesive with thickness of about 25 mm. The thermal conductivity of epoxy adhesive was within 0.05 W/(m·K), much less than that of copper. Epoxy adhesive were also wrapped by a layer of Teflon rape about 5 mm for insulation and protection. The heat loss through the sides and bottom could be neglected.

A platinum resistance temperature detector (PT100) was used to measure the pool bulk temperature. It had a precision of ±0.1 K in the whole test range. A Keithley digital voltmeter (Keithley 2700) with resolution of ±0.1 μV was used to measure the electric potential of thermocouples and resistances of PT100. The precision of thermocouples was ±0.1 K. The atmospheric pressure was measured with a mercury barometer. The power of heaters were measured with a dynamometer which had an accuracy of 0.5%. Experiments were monitored with a Visual Basic program, which could collect data automatically every 10 s.

The magnetic field was produced by two sintered Neodymium-Iron-Boron magnets with dimension of 100 × 50 × 12 mm, and the distance between two magnets was 126 mm. The two magnets were closely attached to two rods fixed along the copper block. Table 2 presents the properties of the magnets at 100 °C. The maximum magnetic flux density on the surface of magnet was about 5000G, which was measured by a Gauss Meter with precision of ±2%. In addition, the magnets were also wrapped by Teflon rape, for the purpose of isolating the nanoparticles in nanofluids.

2.2. Preparation of the nanofluids and heating surfaces

Two kinds of nanoparticles(α-Fe_2O_3 and γ-Fe_2O_3) obtained from Aladdin Inc. were used in the pool boiling experiments. The properties of nanoparticles are shown in Table 3 according to the manufacturing specification. A two-step method was adopted to produce nanofluids [9,22]. First, appropriate mass of nanoparticles and 0.5L deionized water were mixed in a beaker. Then 19.5L deionized water and the mixture were mixed together and homogenized using a ultrasonic cleaner. The process at 500 W/40 kHz would last for five hours. All the 20L nanofluid was used as a working fluid for each pool boiling experiment. Since the concentrations of nanofluids were rather low. A longer and more powerful ultrasonic bath was adopted. In addition, each experiment could be completed within the next five hours, therefore, the nanofluid could be considered stable during the experiment [29,30]. Four concentrations of nanofluids were used in this study, which were 0.005 g/L, 0.025 g/L, 0.050 g/L and 0.100 g/L, all of them were prepared with the same method.

Before each experiment, the heating surface was polished by 5000 grit sandpaper firstly. Then the surface was washed with deionized water and a blow drier was used to blow the residue on the surface away. Fig. 4 presents the roughness profile of the heating surface with $Ra = 0.146$ μm. The red line indicates the quotient of the area above the baseline and the sampling length. The green line indicates the quotient of the area below the baseline and the sampling length.

To minimize the influence of residual nanoparticles on the next experiment, the boiling vessel and the test heater were cleaned with deionized water after each experiment. The Teflon tape was also replaced with new one.

Table 2
Properties of magnets.

Remanence (T)	Coercive force (kA/m)	Magnetic energy product (kJ/m^3)
1.28	1026	370

Table 3
Properties of nanoparticles.

Nanoparticles	α-Fe_2O_3	γ-Fe_2O_3
Average nanoparticle diameter (nm)	30 ± 10	10 ± 5
Purity (%)	99.5	98.8
Density (g/cm^3)	5.24	5.24
Nanoparticle morphology	Spherical	Spherical

2.3. Data reduction and uncertainty analysis

The experiments were conducted in saturated condition at atmospheric pressure close to 97.5 kPa. Before each experiment, the temperature of working fluid was maintained at saturated temperature for 30 min to remove the dissolved gas in the fluid. Then the heat flux increased stepwise from 40 kW/m^2 to 380 kW/m^2. The criterion of stable condition was that the variation of the copper block temperature did not exceed 0.2 K in 100 s, and the final data was the average of 10 sets of data. The same procedure was adopted in each experiment to ensure the repeatability.

As previously mentioned, the heat loss through the sides and bottom was neglected. Accordingly, the heat flux and superheat temperature could be calculated using a one-dimensional Fourier's law of heat conduction as below:

$$q_{21} = \lambda \frac{T_2 - T_1}{x_2 - x_1} \tag{1}$$

$$\Delta T = T_w - T_{sat} = T_1 - \frac{q_{21} x_1}{\lambda} - T_{sat} \tag{2}$$

where ΔT is the difference between the wall temperature and saturated temperature. Hence, the boiling heat transfer coefficient was obtained by Eq. (3):

$$h = \frac{q_{21}}{\Delta T} \tag{3}$$

To determine the heat loss, ϕ was defined as heat loss rate. It was calculated as below:

$$q_{32} = \lambda \frac{T_3 - T_2}{x_3 - x_2} \tag{4}$$

$$\phi = \frac{q_{32} - q_{21}}{q_{32}} \times 100\% \tag{5}$$

As ϕ was always less than 5% during stable condition, the assumption of one-dimensional heat conduction could be proven to be tenable.

According to the method proposed by Kline and McClintock [31], the uncertainty of experimental result $U = U(X_1, X_2, \cdots, X_n)$ could be calculated as:

$$\Delta U = \left[\sum_{i=1}^{n} \left(\frac{\partial U}{\partial X_i} \cdot \Delta X_i \right)^2 \right]^{1/2} \tag{6}$$

The uncertainties of the distance and temperature were 0.1 mm and 0.1 K, respectively. Hence, the maximum uncertainties of heat flux and boiling heat transfer coefficient were 5.6% and 6.0%, respectively.

3. Results and discussion

The pool boiling experiments were conducted with α-Fe_2O_3 and γ-Fe_2O_3 nanofluids at atmospheric pressure. The concentrations of nanoparticles ranged from 0.005 g/L to 0.100 g/L. Two kinds of nonuniform magnetic field induced by two neodymium magnets were applied to study the effects of magnetic field on the pool boiling of water-based nanofluids. The study also investigated the possible mechanisms through the analysis of bubble dynamics.

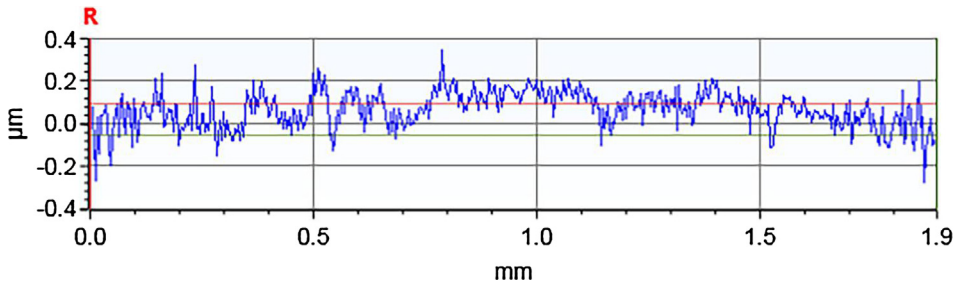

Fig. 4. Roughness profile for the heating surface.

3.1. Validation of experimental system

In order to check the reliability and repeatability of experimental system, the pool boiling experiments of deionized water and 0.005 g/L α-Fe_2O_3 nanofluid were repeated three times on different days. Fig. 5 shows the boiling curves of above-mentioned experiments and the result of Rohsenow correlation. The Rohsenow correlation is expressed as in Eq. (7) [32]:

$$\frac{c_{pl}\Delta t}{r} = C_{wl}\left[\frac{q}{\eta_l r}\sqrt{\frac{\sigma}{g(\rho_l-\rho_v)}}\right]^{0.33} Pr_l^s \tag{7}$$

where c_{pl}, Δt, r, q, η_l, σ, g, ρ_l, ρ_v and Pr are the isobaric heat capacity, superheat temperature, latent heat of the fluid, heat flux, dynamic viscosity of fluid, surface tension, gravitational acceleration, liquid density, vapor density and Prandtl number, respectively. C_{wl} and s are empirical constants. For the polished copper surface, they are equal to 0.013 and 1, respectively. The boiling curves of deionized water were very close to each other, and they agreed well with the Rohsenow correlation. Furthermore, as can be seen from the results of repeated tests, the uncertainty of the superheat temperature of α-Fe_2O_3 nanofluid is nearly 6%. The comparison could validate the experimental system.

3.2. Pool boiling of nanofluids without magnetic field

Considering that most of the previous researchers observed the deterioration of boiling performance at high nanoparticle concentration, the experiments were conducted with α-Fe_2O_3 and γ-Fe_2O_3 nanofluids at lower concentrations (≤0.100 g/L). The boiling heat transfer coefficients of α-Fe_2O_3 and γ-Fe_2O_3 nanofluids with different concentrations are presented in Figs. 6 and 7, respectively. As shown in Fig. 6, the boiling heat transfer coefficient increased about 11% in the 0.005 g/L α-Fe_2O_3 nanofluid, compared with deionized water. However, it showed the performance degradation as the concentration of α-Fe_2O_3 nanofluid increased from 0.005 g/L to 0.100 g/L. For γ-Fe_2O_3 nanofluid, it was found that an

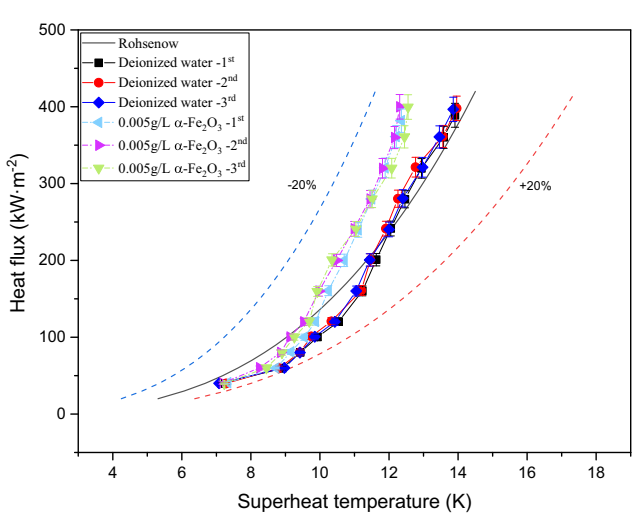

Fig. 5. Boiling curve of deionized water and α-Fe_2O_3 nanofluid (0.005 g/L) compared with Rohsenow correlation.

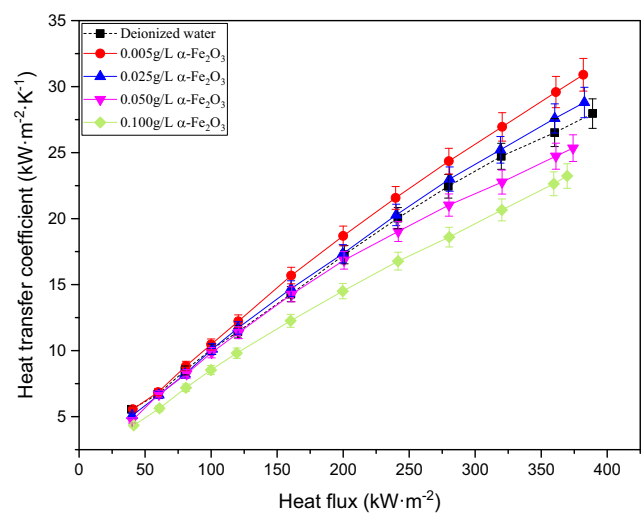

Fig. 6. Boiling heat transfer coefficient according to the concentration of α-Fe_2O_3 nanofluid.

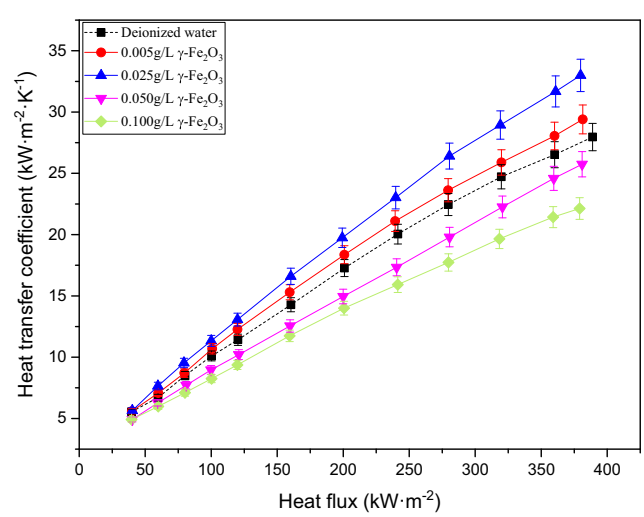

Fig. 7. Boiling heat transfer coefficient according to the concentration of γ-Fe_2O_3 nanofluid.

enhancement of 19% in the boiling heat transfer coefficient was achieved at the concentration of 0.025 g/L. But the boiling heat transfer coefficient significantly declined when the concentration of γ-Fe_2O_3 nanofluid increased from 0.025 g/L to 0.100 g/L.

These results indicated that there was an optimum concentration at which the boiling heat transfer coefficient reached a maximum value. Similar results were reported by previous researchers, and the phenomenon was attributed to the nanoparticles deposited on the heating surface [8,20]. With the evaporation of liquid microlayer, nanoparticles contained in it would gradually deposit on the heating surface [33,34]. At low concentration, if the nanoparticle diameter was smaller than the roughness of heating surface, the existing surface cavities could be split into multiple smaller cavities by the nanoparticles deposited on the surface [16]. Thus, the boiling heat transfer coefficient could be augmented. As the nanoparticle concentration reached a higher level, the nanoparticles could form a porous layer on the heating surface, which caused a decrease in active nucleation site density. Moreover, an extra thermal resistance would occur because of the blocked vapour in the porous layer [35]. Therefore, the boiling heat transfer coefficient firstly increased and then decreased with the increase of nanoparticle concentration. It should be noted that the optimum concentration for α-Fe_2O_3 nanofluid was different from that of γ-Fe_2O_3 nanofluid. Additionally, the γ-Fe_2O_3 nanofluid had lower boiling heat transfer coefficient than that of the α-Fe_2O_3 nanofluid when the nanoparticle concentration was 0.100 g/L. It indicated that the average nanoparticle diameter might also influence the optimum concentration, and the nanoparticles with smaller size could form a smoother porous layer.

It can be seen from the above analysis that the effects of nanoparticles on pool boiling heat transfer might mainly depend on the amount of nanoparticles deposited on the heating surface. If the amount of deposition could be regulated in some ways, it would be possible to have the maximum value of boiling heat transfer coefficient with less cost.

3.3. Pool boiling of nanofluids with the presence of magnetic field

In this experiment, the α-Fe_2O_3 nanoparticles show extremely weak ferromagnetism and γ-Fe_2O_3 nanoparticles exhibit ferrimagnetism [36]. Hence, the characteristics of their nanofluids can be affected by the external magnetic field. Two kinds of magnetic field induced by two magnets were applied. The ANSYS software was used to simulate the spatial distribution of magnetic field in boiling vessel. The magnetic field induced by two magnets that attracted one another was abbreviated as N-S magnetic field in the paper, and that induced by two magnets repelled one another was abbreviated as N-N magnetic field. Fig. 8 shows the spatial distribution of magnetic field lines of N-N and N-S magnetic fields. The tangential direction of magnetic field line is the direction of magnetic field. The density of magnetic field lines reflects the strength of magnetic field. For the N-S magnetic field, the location of maximum magnetic flux density is the center of heating surface. For the N-N magnetic field, the locations of maximum magnetic flux density are four corners of the heating surface. A Gauss Meter was used to measure the magnetic flux density of magnetic field on the heating surface. The maximum magnetic flux density of N-S magnetic field and N-N magnetic field were about 900G and 500G, respectively.

Fig. 9 illustrates the boiling heat transfer coefficients of α-Fe_2O_3 nanofluids with different concentrations in the presence of magnetic field. Since the magnetism of α-Fe_2O_3 nanoparticles was rather weak, the effect of magnetic field on the pool boiling of α-Fe_2O_3 nanofluids was also not obvious. The largest enhancement of 8% was observed for the 0.025 g/L nanofluid under the N-S magnetic field. The N-N magnetic field reduced the boiling heat transfer coefficient of the 0.100 g/L nanofluid about 9%.

Fig. 10 compares the boiling heat transfer coefficient of γ-Fe_2O_3 nanofluids with different concentrations under different magnetic field. The presence of N-S magnetic field reduced the boiling heat transfer coefficient of γ-Fe_2O_3 nanofluids, and the reduction was about 26% for the 0.025 g/L γ-Fe_2O_3 nanofluid. As the increase of nanofluid concentration, the weakening effect of magnetic field diminished gradually. The boiling heat transfer coefficients of 0.100 g/L γ-Fe_2O_3 nanofluid with and without N-S magnetic field were almost identical. For the N-N magnetic field, the enhancement up to 28% was observed when the concentration of γ-Fe_2O_3 nanofluid was 0.050 g/L. However, it reduced the boiling heat transfer coefficient of 0.025 g/L γ-Fe_2O_3 nanofluid by approximately 20%.

3.4. Analysis on the experimental results

This section analyzes the possible mechanisms based on the previous research and the observation of experimental phenomena. The effects of magnetic field can be attributed to three factors: the force acting on the bubble boundary, the magnetic field force on nanoparticle and the magnetic body force on bubble. To simplify the analysis, assuming that the nanoparticles inside the bubble are negligible, because most of the nanoparticles will be absorbed at bubble interface or deposit on the heating surface [12].

The magnetic body force on bubble in an inhomogeneous magnetic field has been analyzed by many previous researchers, and it can be written as [37]:

$$\boldsymbol{F_m} = \frac{1}{2}\mu_0\chi_v\nabla\boldsymbol{H}^2 \tag{8}$$

where $\boldsymbol{F_m}$ is the magnetic force acting on per unit volume, μ_0 is the vacuum permeability and equals $4\pi \times 10^{-7}\mathrm{H}/m$, χ_v and $\boldsymbol{H}$ are the volume susceptibility of water and magnetic field intensity, respectively. Since the deionized water is diamagnetic, χ_v is a negative number. It means that the direction of $\boldsymbol{F_m}$ is opposite to the direction of magnetic field gradient. The magnetic body force mainly influence the velocity and shape of bubble [21]. Therefore, only in the higher heat flux region or under strong magnetic field the effect of magnetic body force is noticeable. If the bubble departure frequency is low, the boiling heat transfer coefficient will not be influenced evidently by the magnetic body force. It can be proved by the results of α-Fe_2O_3 nanofluids with magnetic field (shown in Fig. 9).

The magnetic field force on nanoparticle is essentially a kind of magnetic body force, the direction of which is the same as the direction of magnetic field gradient. While, the force on γ-Fe_2O_3 nanoparticles should be calculated using Maxwell stress tensor rather than Eq. (8), because they have a nonlinear magnetic hysteresis loop. If only magnetic field was taken into consideration, the spatial distribution of γ-Fe_2O_3 nanoparticles is the same with that of magnetic field lines (shown in Fig. 8). In the process of heating γ-Fe_2O_3 nanofluids with magnetic field to saturated condition, the color fading could be observed. It changed from brownish red to light brown. Since the heating process lasted for nearly two hours, the color change of nanofluid was imperceptible when the data were recorded. Moreover, some nanoparticles were absorbed on two magnets. These nanoparticles might alter the distribution of magnetic field. Considering the maximum concentration in the experiment was only 0.100 g/L, this effect could be negligible. The phenomenon indicated that the magnetic field force could cause a directional movement of γ-Fe_2O_3 nanoparticles and reduce the concentration. It should be noted that there were still many nanoparticles dispersing in the base fluid, especially in the fluid microlayer. Because the bubble nucleation, growth and departure

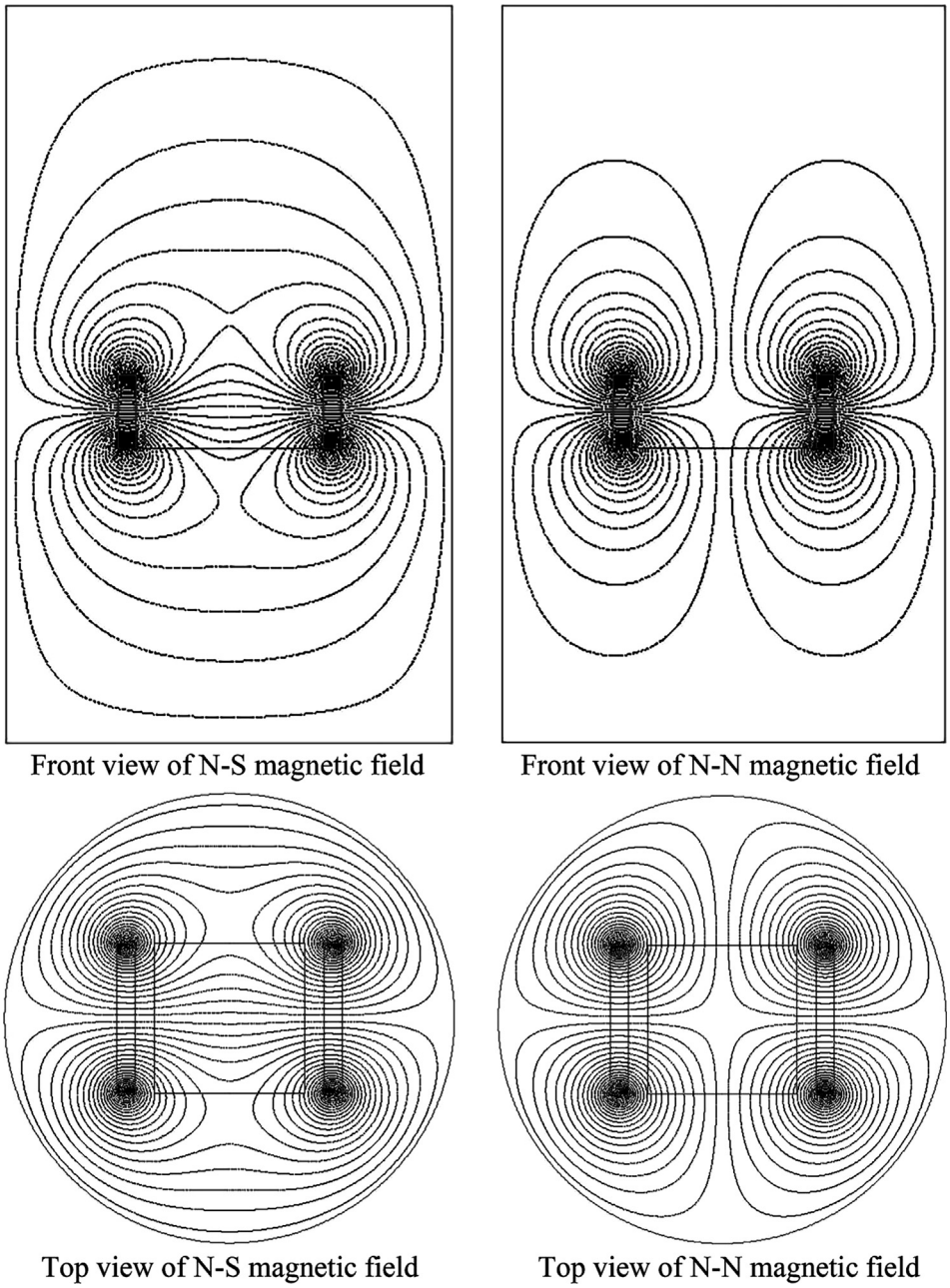

Fig. 8. Schematics of different magnetic field.

could cause a vigorous mixing in nanofluid, it would affect the nanoparticle transport prominently [33]. When an external magnetic field was applied, the distribution of magnetic nanoparticles in nanofluid became considerably complex. It mainly depended on the bubble behavior and the characteristics of magnetic field. Some other factors might also influence it, such as inertia force, Brownian motion and thermophoresis [38].

The force acting on the bubble boundary is caused by the joint effect of magnetic field and nanoparticles. As mentioned above, bubble behaviors could impede the movement of magnetic nanoparticles. Meanwhile, these nanoparticles could also impede the growth of bubbles. In the process of bubble growing, the vapor must overcome the magnetic field force to push the nanoparticles absorbed at bubble boundary. Although it is difficult to calculate the force precisely, a simple model can be used to estimate the effect of this force. As the nanofluid has the volume susceptibility as follows:

$$\chi = c_n\chi_n + (1 - c_n)\chi_v \tag{9}$$

where χ, χ_n and c_n are the volume susceptibility of nanofluid, the volume susceptibility of nanoparticle and the volume concentration of nanoparticle, respectively. The magnetization of nanofluid is $\boldsymbol{M} = \boldsymbol{H}\chi$. The extra pressure ($p^*$) at the bubble boundary can be obtained through the following form suggested by Rosensweig [39]:

$$p^* = \frac{\mu_0 M_n^2}{2} \tag{10}$$

where M_n is the normal component of magnetization. Fig. 11 illustrates the balance of forces at the bubble boundary. It can be seen that p^* impedes the growth of bubble, and the effect of p^* is stronger than that of magnetic body force in the case of higher nanoparticle concentration.

An order of magnitude analysis was carried out to estimate the importance of forces on bubble. Because the 0.050 g/L γ-Fe_2O_3

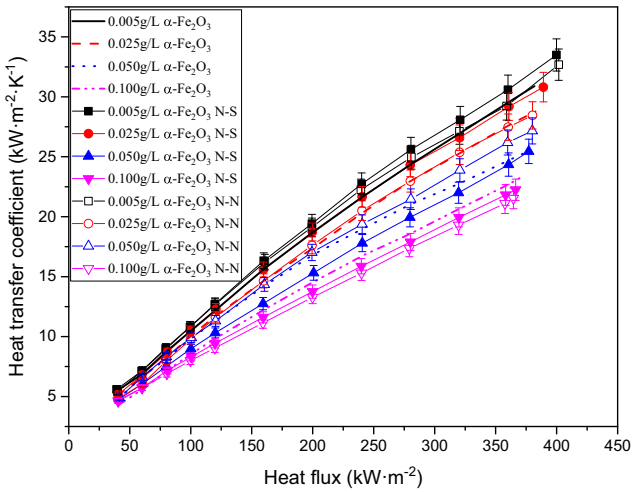

Fig. 9. The boiling heat transfer coefficients of α-Fe_2O_3 nanofluids with different concentrations in the presence of different magnetic field.

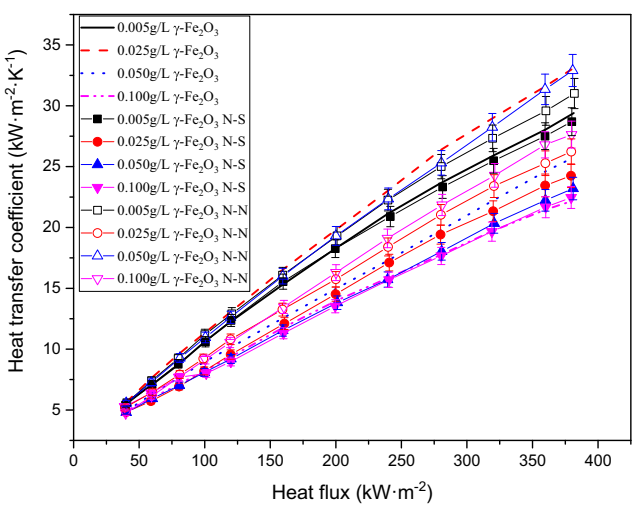

Fig. 10. The boiling heat transfer coefficients of γ-Fe_2O_3 nanofluids with different concentrations in the presence of different magnetic field.

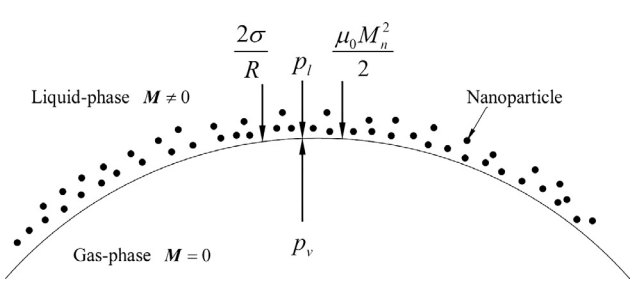

Fig. 11. Balance of forces at the bubble boundary.

nanofluids under N-N magnetic field obtained the maximum heat transfer enhancement, it was representative to carry out the analysis. It was found that the acceleration of bubble caused by magnetic body force was about 0.1 m/s^2. Compared with gravitational acceleration, it was negligible in this research. The extra pressure was about 3 Pa. Assuming the diameter of bubble R ~ 2 mm, it was about one-tenth of 2σ/R. Thus, the extra pressure was more dominant. Because the magnetic field could change the amount of nanoparticles deposition obviously. And the effect of nanoparticles deposition on boiling heat transfer have been discussed in Section 3.2. The experimental results were primarily analyzed from two aspects: the extra pressure and the change of nanoparticles deposition caused by external magnetic field.

Above analysis could provide a plausible explanation for the experimental results. Fig. 12 displays the pool boiling curves for γ-Fe_2O_3 nanofluids (0.005–0.100 g/L) under the N-S magnetic field. It is observed that 0.005 g/L γ-Fe_2O_3 nanofluid has a higher heat flux compared with the other three concentrations. The other three concentrations have a heat transfer performance very close to each other. Because the N-S magnetic field has a stronger intensity, only small amount of nanoparticles could remain in the fluid microlayer. When the concentration reached an equilibrium point, adding more nanoparticles would not have an obvious impact on pool boiling performance unless the amount of nanoparticles was large enough to influence the distribution of magnetic field substantially. Moreover, in most circumstances, the boiling heat transfer coefficient of γ-Fe_2O_3 nanofluids with N-S magnetic field was less than that with N-N magnetic field when their concentrations were the same (shown in Fig. 10). This was due to the N-S magnetic field could cause a higher extra pressure on the bubble boundary, and it reduced the boiling heat transfer coefficient.

Fig. 13 presents the pool boiling curve for deionized water and 0.100 g/L γ-Fe_2O_3 nanofluids with and without magnetic field; Fig. 14 shows the images of heating surface of 0.100 g/L γ-Fe_2O_3 nanofluids. The image (Fig. 14) proved that the magnetic field reduced the amount of nanoparticles deposition significantly. Similar phenomenon was reported by previous literature [26,27]. Due to the nanoparticle coating (Fig. 14(b)), the boiling curve of 0.100 g/L γ-Fe_2O_3 nanofluid without magnetic field moved rightwards significantly, compared with deionized water. Because the nanoparticle coatings were produced by liquid microlayer evaporation, these coatings could demonstrate the location and size of active nucleation sites [6,33,34]. For the 0.100 g/L γ-Fe_2O_3 nanofluid under N-S magnetic field, only the large cavities were activated during boiling because of the extra pressure (Fig. 14(c)), which meant that higher superheat temperature was needed to activate the same size cavity. Thus, the boiling heat transfer coefficient declined notably. For the 0.100 g/L γ-Fe_2O_3 nanofluid with N-N magnetic field, the pool boiling curve was close to that of deionized water although few nanoparticles deposited on the heating surface (Fig. 14(d)). It seemed that the effect of nanoparticles was neutralized by the effect of magnetic field on the whole. Fig. 15 displays the pool boiling curve for γ-Fe_2O_3 nanofluids (0.005–0.100 g/L) with and without the N-N magnetic field. Since

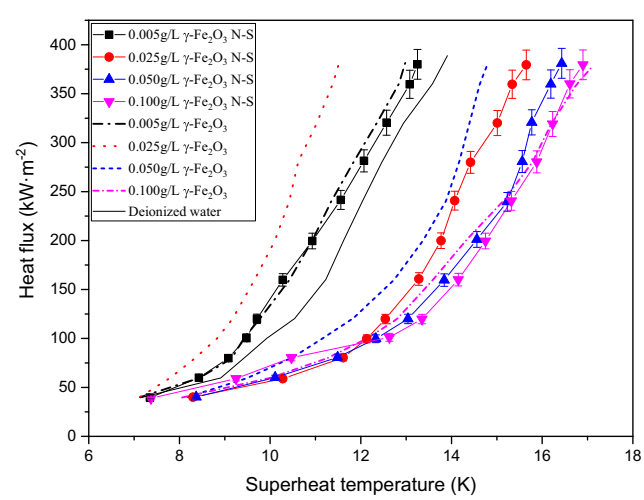

Fig. 12. Boiling curves for γ-Fe_2O_3 nanofluids (0.005–0.100 g/L) with N-S magnetic field.

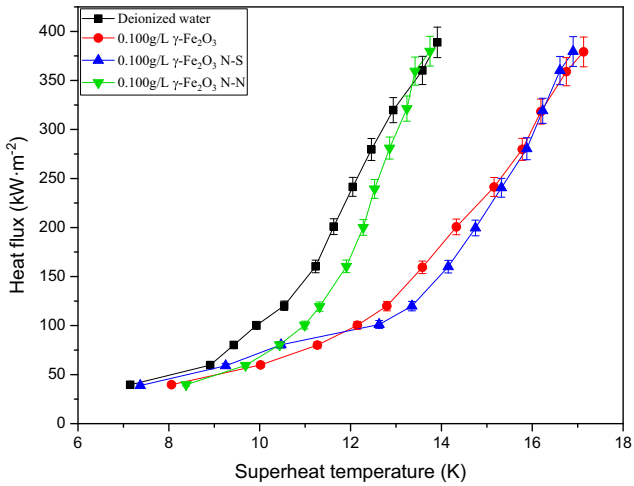

Fig. 13. Boiling curves for deionized water and 0.100 g/L γ-Fe_2O_3 nanofluids under different conditions.

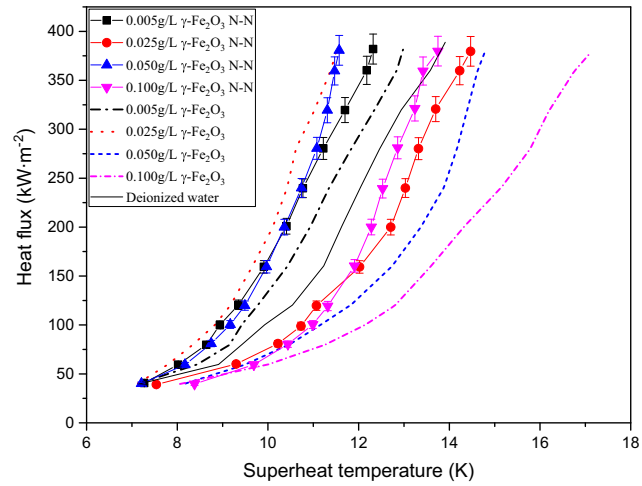

Fig. 15. Boiling curves for γ-Fe_2O_3 nanofluids (0.005–0.100 g/L) with N-N magnetic field.

the magnetic field was weaker and could not remain the actual concentration invariable under the experimental condition, the boiling performance might be influenced by the simultaneous effects of nanoparticles and magnetic field. These nanoparticles could produce many small cavities, but also impede the bubble growth. Thus, the boiling heat transfer coefficient fluctuated with the increase of concentration.

Based on the results and analysis above, the effects of magnetic field on pool boiling of nanofluids can be summarized as follows: The magnetic field can change the local concentration of nanoparticles near the heating surface. An extra pressure on the bubble boundary is produced by the joint effect of external magnetic field and nanoparticles. The effects depend on not only the intensity and

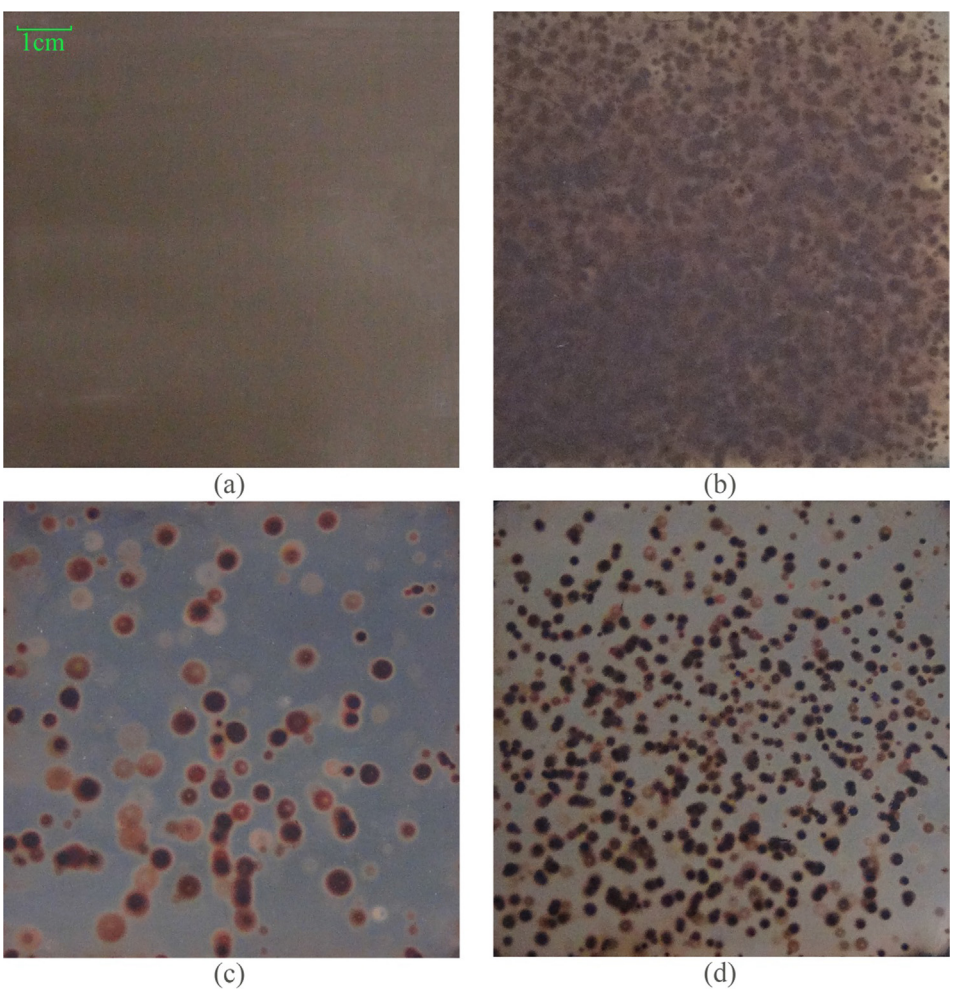

Fig. 14. Images of heat surface for the 0.100 g/L γ-Fe_2O_3 nanofluid: (a) before boiling, (b) after boiling without magnetic field, (c) after boiling with N-S magnetic field, (d) after boiling with N-N magnetic field.

distribution of magnetic field, but also the magnetism and concentration of nanoparticles. Thus, controlling the boiling process of magnetic nanofluids by external magnetic field is feasible. If the maximum magnetic flux density occurs on the heating surface, the local concentration near the surface can be increased remarkably, which means fewer nanoparticles are needed to reach the optimum concentration. Meanwhile, the downward gradient of magnetic field can enhance the boiling heat transfer. Although the extra pressure will deteriorate the boiling performance, its negative effects can be minimized by adjusting the magnetic field intensity. If many nanoparticles have deposited on the heating surface and deteriorated the boiling heat transfer, adopting a suitable magnetic field can be an effective way to remove them.

4. Conclusions

In this paper, experiments were conducted using water-based nanofluids containing α-Fe_2O_3 and γ-Fe_2O_3 nanoparticles in the presence of different magnetic field at atmospheric pressure. The primary objective of the investigation was to investigate the effects of magnetic field on pool boiling characteristics of nanofluids. The concentration of nanoparticles ranged from 0.005 g/L to 0.100 g/L. And these effects were attributed to three factors: the magnetic body force on bubble, the force acting on the bubble boundary and the magnetic field force on nanoparticle. The results can be summarized as below:

(1) The effects of magnetic field were dependent on the characteristics of magnetic field and nanofluids. The effects was rather weak for the pool boiling of α-Fe_2O_3 nanofluids and that with lower concentrations of γ-Fe_2O_3 nanofluid. When the concentration was higher, the magnetic field could change the actual concentration of γ-Fe_2O_3 nanoparticles.
(2) Compared to the effects of nanoparticles on pool boiling, the magnetic field plays a dominant role when the intensity of field is strong. In the weak magnetic field, the boiling performance was influenced by the simultaneous effect of nanoparticles and magnetic field. For the 0.050 g/L γ-Fe_2O_3 nanofluid, the enhancement in boiling heat transfer coefficient was up to 28% due to the presence of magnetic field induced by two mutually exclusive magnets.
(3) There is an extra pressure on the bubble boundary, which is produced by the joint effect of external magnetic field and nanoparticles. The extra pressure will impede the growth of bubble and deteriorate the heat transfer.
(4) There is an optimum concentration in which the enhancement of pool boiling heat transfer of nanofluid can be maximized. It might be correlated with the average diameter of nanoparticles. For the 0.025 g/L γ-Fe_2O_3 nanofluid, the enhancement in the boiling heat transfer coefficient was up to 19% compared with deionized water.

Conflict of interest

The authors declared that there is no conflict of interest.

Acknowledgment

This work was supported by the National Key R&D Program of China (No.2016YFB0601200), National Natural Science Foundation of China (51776160) and Open Fund of the Key Laboratory of Thermo-Fluid Science and Engineering of MOE.

References

[1] D. Ciloglu, A. Bolukbasi, A comprehensive review on pool boiling of nanofluids, Appl. Therm. Eng. 84 (2015) 45–63.
[2] X. Fang, Y. Chen, H. Zhang, W. Chen, A. Dong, R. Wang, Heat transfer and critical heat flux of nanofluid boiling: a comprehensive review, Renew. Sustain. Energy Rev. 62 (2016) 924–940.
[3] J. Ham, H. Kim, Y. Shin, H. Cho, Experimental investigation of pool boiling characteristics in Al_2O_3 nanofluid according to surface roughness and concentration, Int. J. Therm. Sci. 114 (2017) 86–97.
[4] L.L. Manetti, M.T. Stephen, P.A. Beck, E.M. Cardoso, Evaluation of the heat transfer enhancement during pool boiling using low concentrations of Al_2O_3-water based nanofluid, Exp. Therm Fluid Sci. 87 (2017) 191–200.
[5] A. Nikulin, O. Khliyeva, N. Lukianov, V. Zhelezny, Y. Semenyuk, Study of pool boiling process for the refrigerant R11, isopropanol and isopropanol/Al_2O_3 nanofluid, Int. J. Heat Mass Transf. 118 (2018) 746–757.
[6] M.Z. Sulaiman, D. Matsuo, K. Enoki, T. Okawa, Systematic measurements of heat transfer characteristics in saturated pool boiling of water-based nanofluids, Int. J. Heat Mass Transf. 102 (2016) 264–276.
[7] M. Karimzadehkhouei, M. Shojaeian, K. Şendur, M.P. Mengüç, A. Koşar, The effect of nanoparticle type and nanoparticle mass fraction on heat transfer enhancement in pool boiling, Int. J. Heat Mass Transf. 109 (2017) 157–166.
[8] Y. Hu, H. Li, Y. He, Z. Liu, Y. Zhao, Effect of nanoparticle size and concentration on boiling performance of SiO_2 nanofluid, Int. J. Heat Mass Transf. 107 (2017) 820–828.
[9] A.V. Minakov, M.I. Pryazhnikov, D.V. Guzei, G.M. Zeer, V.Y. Rudyak, The experimental study of nanofluids boiling crisis on cylindrical heaters, Int. J. Therm. Sci. 116 (2017) 214–223.
[10] S.N. Shoghl, M. Bahrami, M. Jamialahmadi, The boiling performance of ZnO, α-Al_2O_3 and MWCNTs/water nanofluids: an experimental study, Exp. Therm Fluid Sci. 80 (2017) 27–39.
[11] L.W. Fan, J.Q. Li, Y.Z. Wu, L. Zhang, Z.T. Yu, Pool boiling heat transfer during quenching in carbon nanotube (CNT)-based aqueous nanofluids: effects of length and diameter of the CNTs, Appl. Therm. Eng. 122 (2017) 555–565.
[12] X. Quan, D. Wang, P. Cheng, An experimental investigation on wettability effects of nanoparticles in pool boiling of a nanofluid, Int. J. Heat Mass Transf. 108 (2017) 32–40.
[13] R.R. Souza, J.C. Passos, E.M. Cardoso, Influence of nanoparticle size and gap size on nucleate boiling using HFE7100, Exp. Therm Fluid Sci. 59 (2014) 195–201.
[14] I.S. Kiyomura, L.L. Manetti, A.P. Cunha, G. Ribatski, E.M. Cardoso, An analysis of the effects of nanoparticles deposition on characteristics of the heating surface and ON pool boiling of water, Int. J. Heat Mass Transf. 106 (2017) 666–674.
[15] M.R. Salimpour, A. Abdollahi, M. Afrand, An experimental study on deposited surfaces due to nanofluid pool boiling: comparison between rough and smooth surfaces, Exp. Therm Fluid Sci. 88 (2017) 288–300.
[16] G. Harish, V. Emlin, V. Sajith, Effect of surface particle interactions during pool boiling of nanofluids, Int. J. Therm. Sci. 50 (12) (2011) 2318–2327.
[17] B. Stutz, C.H.S. Morceli, M.F. Silva, S. Cioulachtjian, J. Bonjour, Influence of nanoparticle surface coating on pool boiling, Exp. Therm Fluid Sci. 35 (2011) 1239–1249.
[18] M. Sheikhbahai, M.N. Esfahany, N. Etesami, Experimental investigation of pool boiling of Fe_3O_4/ethylene glycol-water nanofluid in electric field, Int. J. Therm. Sci. 62 (2012) 149–153.
[19] E. Salari, S.M. Peyghambarzadeh, M.M. Sarafraz, F. Hormozi, V. Nikkhah, Thermal behavior of aqueous iron oxide nano-fluid as a coolant on a flat disc heater under the pool boiling condition, Heat Mass Transf. 53 (1) (2017) 265–275.
[20] A. Abdollahi, M.R. Salimpour, N. Etesami, Experimental analysis of magnetic field effect on the pool boiling heat transfer of a ferrofluid, Appl. Therm. Eng. 111 (2017) 1101–1110.
[21] J. Ishimoto, M. Okubo, S. Kamiyama, M. Higashitani, Bubble behavior in magnetic fluid under a nonuniform magnetic field, JSME Int. J. Ser. B 38 (3) (1995) 382–387.
[22] J.H. Lee, T. Lee, Y.H. Jeong, Experimental study on the pool boiling CHF enhancement using magnetite-water nanofluids, Int. J. Heat Mass Transf. 55 (2012) 2656–2663.
[23] H.H. Khoshmehr, A. Saboonchi, M.B. Shafii, N. Jahani, The study of magnetic field implementation on cylinder quenched in boiling ferro-fluid, Appl. Therm. Eng. 64 (2014) 331–338.
[24] L. Junhong, G. Jianming, L. Zhiwei, L. Hui, Experiments and mechanism analysis of pool boiling heat transfer enhancement with water-based magnetic fluid, Heat Mass Transf. 41 (2) (2004) 170–175.
[25] M. Şeşen, Y. Tekşen, B. Şahin, K. Şendur, M.P. Mengüç, A. Koşar, Boiling heat transfer enhancement of magnetically actuated nanofluids, Appl. Phys. Lett. 102 (16) (2013) 1–5.
[26] M. Shojaeian, M.M. Yildizhan, O. Coşkun, E. Ozkalay, Y. Tekşen, M.A. Gulgun, H. F.Y. Acar, A. Koşar, Investigation of change in surface morphology of heated surfaces upon pool boiling of magnetic fluids under magnetic actuation, Mater. Res. Express 3 (9) (2016) 096102.
[27] M.R. Özdemir, A.K. Sadaghiani, A.R. Motezakker, S.S. Parapari, H.S. Park, H.Y. Acar, A. Koşar, Experimental studies on ferrofluid pool boiling in the presence of external magnetic force, Appl. Therm. Eng. 139 (2018) 598–608.
[28] L. Chen, Z. Xu, H. Dai, S. Zhang, Facile synthesis and magnetic properties of monodisperse Fe_3O_4/silica nanocomposite microspheres with embedded

structures via a direct solution-based route, J. Alloy. Compd. 497 (1–2) (2010) 221–227.
[29] L. Colla, L. Fedele, M. Scattolini, S. Bobbo, Water-based nanofluid characterization: thermal conductivity and viscosity measurements and correlation, Adv. Mech. Eng. 2015 (2012) 293–298.
[30] I. Nurdin, I.I. Yaacob, M.R. Johan, Enhancement of thermal conductivity and kinematic viscosity in magnetically controllable maghemite (γ-Fe_2O_3) nanofluids, Exp. Therm. Fluid Sci. 77 (2016) 265–271.
[31] S.J. Kline, F.A. McClintock, Describing uncertainties in single-sample experiments, Mech. Eng. 75 (1953) 3–8.
[32] J.P. Hartnett, W.M. Rohsenow, Y. Cho, Handbook of heat transfer. Handbook of heat transfer, vol. 1, third ed., in: J.P. Hartnett, Warren M. Rohsenow, McGraw-Hill, New York, 1998.
[33] S.J. Kim, I.C. Bang, J. Buongiorno, L.W. Hu, Surface wettability change during pool boiling of nanofluids and its effect on critical heat flux, Int. J. Heat Mass Transf. 50 (19–20) (2007) 4105–4116.
[34] S.M. Kwark, R. Kumar, G. Moreno, J. Yoo, S.M. You, Pool boiling characteristics of low concentration nanofluids, Int. J. Heat Mass Transf. 53 (5–6) (2010) 972–981.
[35] Z. Shahmoradi, N. Etesami, M.N. Esfahany, Pool boiling characteristics of nanofluid on flat plate based on heater surface analysis, Int. Commun. Heat Mass Transf. 47 (2013) 113–120.
[36] R. Zboril, M. Mashlan, D. Petridis, Iron(III) oxides from thermal processes-synthesis, structural and magnetic properties, Mössbauer spectroscopy characterization, and applications, Chem. Mater. 14 (3) (2002) 969–982.
[37] L. Yang, J. Ren, Y. Song, Z. Guo, Free convection of a gas induced by a magnetic quadrupole field, J. Magn. Magn. Mater. 261 (3) (2003) 377–384.
[38] M. Şeşen, Y. Tekşen, K. Şendur, M.P. Menguc, H. Ozturk, H.F.Y. Acar, A. Kosar, Heat transfer enhancement with actuation of magnetic nanoparticles suspended in a base fluid, J. Appl. Phys. 112 (6) (2012) 1972.
[39] R.E. Rosensweig, Magnetic fluids, Annu. Rev. Fluid Mech. 19 (1) (1987) 437–461.